The evolution of Titan's detached haze layer near equinox in 2009

Article in Geophysical Research Letters · March 2011
DOI: 10.1029/2011GL046843 · Source: OAI

8 authors, including:

Robert West
California Institute of Technology

Jonathan Balloch
Georgia Institute of Technology

Panayotis Lavvas
Université de Reims Champagne-Ardenne

Ralph Detlef Lorenz
Johns Hopkins University

The evolution of Titan's detached haze layer near equinox in 2009

Robert A. West,[1] Jonathan Balloch,[1] Philip Dumont,[1] Panayotis Lavvas,[2] Ralph Lorenz,[3]
Pascal Rannou,[4,5] Trina Ray,[1] and Elizabeth P. Turtle[3]

Received 21 January 2011; revised 11 February 2011; accepted 15 February 2011; published 31 March 2011.

[1] Saturn's moon Titan has a massive atmosphere laden with layers of photochemical haze. We report a recent dramatic change in the vertical structure of this haze, with a persistent 'detached' layer dropping in altitude from over 500 km to only 380 km between 2007 and 2010. The detached haze layer appears to be a well-defined tracer for Titan's meridional stratospheric circulation, models of which suggest that a pole-to-pole meridional cell weakens during equinox as solar heating becomes more symmetric. These measurements connect the Cassini observations with those made by Voyager almost one seasonal cycle earlier. They place detailed constraints on the seasonal circulation, on the sources of photochemical aerosols, on the microphysical processes and on the complex interplay of these components. **Citation:** West, R. A., J. Balloch, P. Dumont, P. Lavvas, R. Lorenz, P. Rannou, T. Ray, and E. P. Turtle (2011), The evolution of Titan's detached haze layer near equinox in 2009, *Geophys. Res. Lett.*, *38*, L06204, doi:10.1029/2011GL046843.

1. Background

[2] Titan's extensive photochemical haze shapes the satellite's appearance at visible wavelengths, plays a critical role in atmospheric energy balance, thermal structure and dynamics, is a sink for photochemical reactions and a source for surface organic material and contains important clues to the nature of the atmospheric circulation and seasonal variations [see *Rannou et al.*, 2002; *Tomasko et al.*, 2008a; *Roman et al.*, 2009]. *Liang et al.* [2007] reported evidence for haze opacity at ultraviolet wavelengths up to 1000 km altitude and *Waite et al.* [2007] found evidence for haze formation starting with photolysis of methane and nitrogen near that altitude and deeper.

[3] Images of Titan from Voyagers 1 and 2 [see *Smith et al.*, 1981, 1982] revealed a hemispheric contrast and a nearly global 'detached' (forming a distinct local maximum) haze layer near 350 km altitude at latitudes outside of the polar vortex. To account for the hemispheric contrast *Sromovsky et al.* [1981] proposed a seasonal mechanism with a substantial phase lag. Here we report Cassini imaging observations of a large seasonal change in the altitude of the detached haze with a very different phase behavior. The high altitude haze and the albedo are likely not directly linked because they are formed at different altitudes, but the fact they each have seasonal variations may suggest a common root in changes in the dynamics.

2. Observations

[4] In the discussion that follows we address the haze structure at latitudes outside of the polar vortex region whose boundary was near +55° during the Cassini observations.

[5] We measured the altitude of Titan's detached haze in 81 Cassini Imaging Science Subsystem (ISS) images from day 297 (23 October) of 2004 to day 219 (7 August) of 2010. The images show Titan's full disk with image scales ranging from 6.3 to 16.3 km/pixel, plus one image at 22.5 km/pixel. Images were obtained in the ISS UV3, blue and green filters over a range of phase angles from 0.8° to 163.7°. Determination of the altitude of the detached haze was found to be insensitive to filter or phase angle. Figure 1 shows a sample of two images that happen to be at high phase angles similar to the primary Voyager image analyzed by *Rages and Pollack* [1983].

[6] Beginning in 2004 the local maximum brightness produced by the detached haze could be fit, with one-pixel residuals, by a circle centered on Titan. By day 320 of 2008 (Equinox −269 days) the haze became noticeably non-circular. Maximum altitudes always occur at or near the equator and these are shown in Figure 2, along with the difference between maximum and minimum altitudes for a subset of the images. At equinox on day 223 (11 August) 2009 the difference reached a maximum value (30 km) and then diminished toward the value reported by *Rages and Pollack* [1983] for the Voyager case, also shown in Figure 2.

[7] To better understand how limb intensity gives information about haze density vertical profiles we derived haze extinction profiles from limb intensity profiles with the help of a scalar radiative transfer model for intensity which operates in a spherical shell geometry and handles arbitrary phase functions and single and multiple scattering separately. The multiply-scattered field used phase function truncation. The procedure is an adaptation of the classic Lambda Iteration approach employed for stellar atmospheres. The algorithm uses acceleration schemes due to *Ng* [1974] and *Auer* [1987].

[8] Figure 3 illustrates how vertical profiles of the haze change with time. To a first approximation a time-independent component of the haze density decreases exponentially in altitude with a scale height of 47 km (the dotted lines), similar to the gas scale height (N_2 pressure scale height is in the range 47–53 km for temperature in the range 150–170 K

[1]Jet Propulsion Laboratory, California Institute of Technology, Pasadena, California, USA.
[2]Lunar and Planetary Laboratory, University of Arizona, Tucson, Arizona, USA.
[3]Johns Hopkins University Applied Physics Laboratory, Laurel, Maryland, USA.
[4]GSMA, UMR 6089, CNRS, Université de Reims Champagne-Ardenne, Reims, France.
[5]LATMOS, UMR 8190, CNRS, Université de Versailles St-Quentin, Verrières-le-Buisson, France.

0094-8276/11/2011GL046843

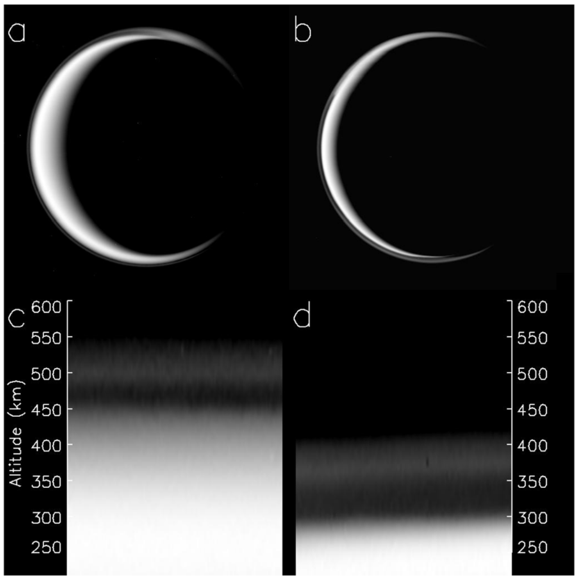

Figure 1. Two of the 81 images used in this study appear in Figures 1a and 1b. Solar illumination is from the left and image scale is the same in both. (a) Frame N1525327324, taken well before equinox on day 123 of 2006, with the north pole at a 32° angle clockwise from vertical. (b) Frame N1648925013 taken on day 92 of 2010, several months after equinox, with north near vertical. Both were obtained with the UV3 filter (effective wavelength 343 nm). The phase angles (146. 8° and 153.3° in Figures 1a and 1b, respectively) are similar to that for the Voyager 2 image analyzed by *Rages and Pollack* [1983]. (c and d) Magnification of the region near the limb at the sub-solar latitude in the corresponding Figures 1a and 1b. Solar illumination is from the top. Brightness is shown on a logarithmic scale to compress the dynamic range and make visible the detached haze. I/F (where I is intensity and πF is the incident solar flux) can be judged from the plots in Figure 3.

relevant to these altitudes as reported by *Fulchignoni et al.* [2005]). Referencing to the dotted lines in Figure 3 suggests that the temporal change is due primarily to an altitude drop in the haze local minimum (a gap) rather than the altitude change of a local maximum. As time passes the width of the gap increases, as measured by the vertical span of the region at 90% or less of the corresponding dotted lines in Figure 3. A prominent local maximum above 500 km is apparent in the 2006 profile but the local maximum near 400 km in the 2010 image does not rise above the time-independent reference profile shown by the associated dotted line. The 2010 profile suggests that it is the evolution of the location and width of the local minimum which is important for seasonal models of haze evolution.

[9] Discovery of the altitude of the detached haze as seen in Cassini images in 2004 prompted *Porco et al.* [2005] and *Lorenz et al.* [2009] to predict seasonal variations in the altitude of the detached haze. Our data provide new detail on the time and rate at which the phenomenon occurs. A striking feature is that the change occurs most rapidly quite close to equinox, providing strong support for the idea that a seasonal dynamical or coupled dynamical/photochemical/microphysical process is responsible.

3. Haze Production, Dynamical Models and Seasonal Factors

[10] Three potentially important processes are changing on Titan with various time scales. First, variations in the flux of solar ultraviolet light and precipitating particles in Saturn's magnetosphere may modulate the photochemical production of organics in Titan's thermosphere and stratosphere. Global UV fluxes have no strong correlation with the equinox. However, UV flux at high latitude is correlated with the equinox (which is the only time neither pole is in shadow), so equinox illumination and photochemical production coupled with the meridional circulation may play an important role. Second, Saturn's orbit around the sun is eccentric, with periapsis (9AU; Ls = 280, most recently in 2003) near southern summer solstice (Ls = 270; 2002) much closer than

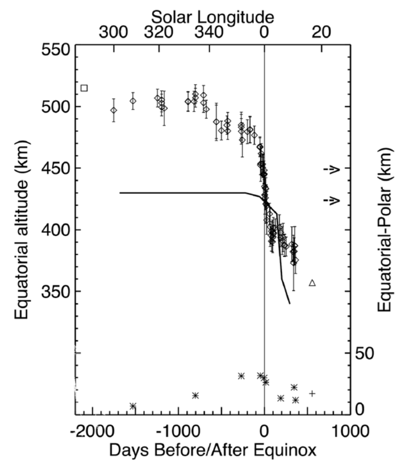

Figure 2. Measurements from Cassini ISS images of the equatorial altitude of the peak brightness of the detached haze are plotted as diamonds with 1-pixel error bars (left ordinate scale). Peak brightness is defined as the prominent local maximum in I/F as a function of altitude. At the spatial resolution of the images used in this study the 'detached haze' appears to be a single layer. The triangle at equinox +555 represents Voyager measurements from *Rages and Pollack* [1983] who found altitudes from 340 +− 10 to 357 +− 5 km over a range of latitudes with the highest value at the equator and the lowest at the pole. The square at equinox-2097 days shows the altitude of a strong temperature inversion reported by *Sicardy et al.* [2006] inferred from stellar occultation data. *Lavvas et al.* [2009] proposed that the inversion is generated by aerosol heating associated with the detached haze layer. Two more temperature inversions were reported by *Sicardy et al.* [1999] from occultation data obtained in 1989 (3413 days after the 1980 equinox at solar longitude 109°) and are indicated by the arrows. The solid curve is the trajectory of the altitude at the maximum of the detached haze at the equator for the model of *Rannou et al.* [2002]. Equatorial – polar altitude differences are plotted against the right ordinate scale; the + symbol refers to a measurement by Rages and Pollack (for polar latitude 75 S). The * symbols are measured from Cassini ISS images.

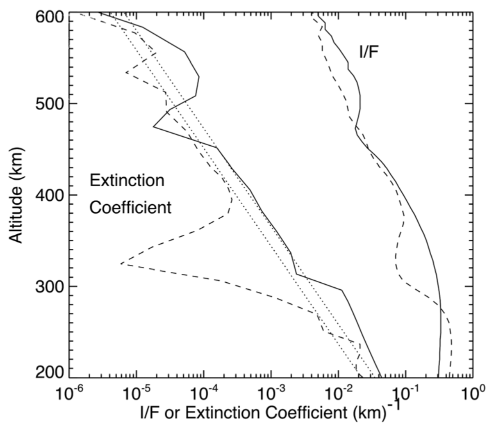

Figure 3. Haze extinction vertical profiles retrieved from images shown in Figure 1 are plotted along with I/F for a radial profile near the sub-solar latitude. The solid curve is for image N1525327324 (day 123 of 2006) and the dashed curve is for image N1648925013 (day 92 of 2010). The retrievals used data from a wide range of latitudes south of 55° and are therefore latitude averages. The retrievals used a highly forward-peaked phase function from the tables of *Tomasko et al.* [2008b] and single-scattering albedo 0.7. They are insensitive to aerosols deeper than about 200-250 km. The I/F plot shows one major local minimum with a corresponding local maximum just above it. Those are the features we address in this paper. Any other local minimum or maximum may or may not be real pending further investigation. Extinction coefficient over a significant range of altitudes follows an exponential line with scale height 46.6 km (dotted lines), except for the prominent local minimum near 320 km in 2010 and the local minimum near 470 km and local maximum near 505 km in 2006. The gas pressure scale height for N_2 at 500 km would be between 46.9 and 53.2 km for temperature in the range 150 to 170 K as reported by *Fulchignoni et al.* [2005].

apoapsis (10AU; Ls = 100, 2018). Titan is presently receding from the sun and the total solar input is declining slowly, so at altitudes above ~200 km (where the radiative time constant is ~1 year [*Flasar et al.*, 1981]) the atmosphere may be cooling and therefore shrinking. However, this change is not abrupt. Finally, the solar latitude is changing due to the 26.5° obliquity of Titan. The equinox period is when the solar latitude changes most rapidly, having moved from −20° in 2006 to 0.2° at the time of our last measurement.

[11] Models of Titan's meridional circulation [e.g., *Rannou et al.*, 2002] show that solar heating drives a pole-to-pole cell for almost half a Titan year, with rising air in the summer hemisphere. As the sun moves into the other hemisphere each equinox, this flow weakens (possibly with a transient symmetric two-cell flow for a year or two) and reverses. This profound change in atmospheric flow is plausibly responsible for the dramatic change in the altitude of the detached haze.

[12] *Rannou et al.* [2002] used an axially symmetric version of a general circulation model to simulate seasonal variations on Titan. They coupled this to an aerosol microphysical model to account for radiative heating/cooling by aerosols and to use aerosols as a tracer to compare with data. One detail from the model is shown in Figure 2. A relative maximum (meaning a local maximum in altitude) in equatorial haze density moves lower in altitude after equinox, similar to the data. However, the altitude of the local maximum is too low and the rapid part of the collapse is delayed about three hundred days relative to the observation. The shifted timing in the model could be due to the low altitude of the detached haze compared to observation with an associated longer response time to seasonal forcing. Intrinsic limitations of the two-dimensional approximation in the model (dynamics, parameterization of waves and radiative transfer) and a limitation in the vertical range of the model may also contribute. A more serious concern is that the local minimum vanishes or is very weak in the model about 300 days after equinox, whereas the data show a strong local minimum (Figures 1b and 1d and the dashed curve in Figure 3).

[13] A mechanism proposed by *Lavvas et al.* [2009] produces the detached haze layer in a very different way that does not depend on dynamical transport. In that model the location of the detached haze is determined by aerosol microphysics – it is the altitude where the monomers sedimenting from higher altitudes coagulate to form aggregates [*Tomasko et al.*, 2008b; *Tomasko and West*, 2009; *Tomasko et al.*, 2009]: a shape and size transition. In this model the altitude where the detached layer resides is sensitive to aerosol formation rates, which are tied to higher-altitude chemical reactions in the gas phase.

[14] A key impetus for the microphysical model of *Lavvas et al.* [2009] is that the detached layer is nearly spherically symmetric around Titan at all latitudes outside of the winter polar vortex region. It is difficult to see how advection along streamlines could produce this feature. In a pole-to-pole circulation as proposed by *Rannou et al.* [2002] the streamlines in the upwelling summer high latitudes trend toward vertical and should produce a corresponding trend in the detached layer. However, the Lavvas et al. microphysical description of the detached layer does not account for time variations. Although the microphysical idea behind the production of a detached layer may remain viable but it must be coupled with a mechanism (almost certainly a dynamical one) responsible for the altitude variation and must be evaluated primarily in light of other observations or theoretical arguments.

[15] To better understand the processes responsible for the collapse of the haze it would be helpful to know at what phase in the seasonal cycle the detached haze will return to the 500-km altitude range. A few observations from the ground are relevant to this issue. *Lavvas et al.* [2009] argued that radiative heating in the detached layer is responsible for a temperature feature at the same altitude in stellar occultation retrievals by *Sicardy et al.* [1999, 2006]. A 2003 temperature feature from stellar occultation [*Sicardy et al.*, 2006] aligns with the Cassini measurements beginning in 2004. Temperature inversions observed in 1989 (3413 days after the 1980 vernal equinox) indicate aerosol layers near 420 and 450 km (the arrows in Figure 2). If these features are tracking haze layers it is unclear how to place them into a seasonal model for haze evolution. More data between the equinoxes are needed.

[16] The dynamical model by *Rannou et al.* [2002] predicts the fate of the detached haze over a full seasonal cycle. With the turnover of the stratospheric circulation at equinox, the broad ascending branch of the stratospheric cell moves from the southern hemisphere to the northern hemisphere

within few terrestrial years. The change in the wind pattern, especially in the ascending branch in the summer hemisphere, breaks the equilibrium between the aerosol settling speed and the ascending wind speed, producing a temporary disappearance of the detached haze beginning about 300 days after equinox. After about three years, the opposite circulation is installed and the detached haze will gradually emerge again near its initial altitude around year 2013, to reach a stable state (after 2016). This sequence of events occurs twice each Kronian year. The two periods between equinoxes are not symmetric due to orbital eccentricity. This may explain the altitudes of temperature inversions observed by *Sicardy et al.* [1999, 2006] at opposite seasons with the occultations in 1989 and 2003. Cassini Images to be obtained through the end of mission at solstice in 2017 will test this prediction.

[17] **Acknowledgments.** Part of this work was performed by the Jet Propulsion Laboratory, California Institute of Technology, funded by the NASA Astrobiology Institute and by the Cassini Project. RL was supported by the NASA Cassini Data Analysis Program. We thank M. Evans for work on the optical navigation of one image, and C. Porco who helped with an early version of the paper.

[18] The Editor thanks two anonymous reviewers for their assistance in evaluating this paper.

References

Auer, L. H. (1987), Acceleration of convergence, in *Numerical Radiative Transfer*, edited by W. Kalkofen, p. 101, Cambridge Univ. Press, Cambridge, U. K.

Flasar, F. M., R. E. Samuelson, and B. J. Conrath (1981), Titan's atmosphere: Temperature and dynamics, *Nature*, *292*, 693–698, doi:10.1038/292693a0.

Fulchignoni, M., et al. (2005), In situ measurements of the physical characteristics of Titan's environment, *Nature*, *438*, 785–791, doi:10.1038/nature04314.

Lavvas, P., R. V. Yelle, and V. Vuitton (2009), The detached haze layer in Titan's mesosphere, *Icarus*, *201*, 626–633, doi:10.1016/j.icarus.2009.01.004.

Liang, M. C., Y. L. Yung, and D. E. Shemansky (2007), Photolytically generated aerosols in the mesosphere and thermosphere of Titan, *Astrophys. J.*, *661*, L199–L202, doi:10.1086/518785.

Lorenz, R. D., M. E. Brown, and M. Flasar (2009), Seasonal change on Titan, in *Titan From Cassini-Huygens*, edited by R. H. Brown, J.-P. Lebreton, and J. H. Waite, pp. 353–372, Springer, New York, doi:10.1007/978-1-4020-9215-2_14.

Ng, K. C. (1974), Hypernetted chain solutions for classical one-component plasma up to $\Gamma = 7000$, *J. Chem. Phys.*, *61*, 2680–2689, doi:10.1063/1.1682399.

Porco, C., et al. (2005), Imaging of Titan from the Cassini spacecraft, *Nature*, *434*, 159–168, doi:10.1038/nature03436.

Rages, K., and J. B. Pollack (1983), Vertical distribution of scattering hazes in Titan's upper atmosphere, *Icarus*, *55*, 50–62, doi:10.1016/0019-1035(83)90049-0.

Rannou, P., F. Hourdin, and C. P. McKay (2002), A wind origin for Titan's haze structure, *Nature*, *418*, 853–856, doi:10.1038/nature00961.

Roman, M. T., R. A. West, D. J. Banfield, P. J. Gierasch, R. K. Achterberg, C. A. Nixon, and P. C. Thomas (2009), Determining the tilt in Titan's north-south albedo asymmetry from Cassini images, *Icarus*, *203*, 242–249, doi:10.1016/j.icarus.2009.04.021.

Sicardy, B., et al. (1999), The structure of Titan's stratosphere from the 28 Sgr occultation, *Icarus*, *142*, 357–390, doi:10.1006/icar.1999.6219.

Sicardy, B., et al. (2006), The two Titan stellar occultations of 14 November 2003, *J. Geophys. Res.*, *111*, E11S91, doi:10.1029/2005JE002624.

Smith, B. A., et al. (1981), Encounter with Saturn: Voyager 1 imaging science results, *Science*, *212*, 163–191, doi:10.1126/science.212.4491.163.

Smith, B. A., et al. (1982), A new look at the Saturn system: The Voyager 2 images, *Science*, *215*, 504–537, doi:10.1126/science.215.4532.504.

Sromovsky, L. A., V. E. Suomi, J. B. Pollack, R. J. Krauss, S. S. Limaye, T. Owen, H. E. Revercomb, and C. Sagan (1981), Implications of Titan's north–south brightness asymmetry, *Nature*, *292*, 698–702, doi:10.1038/292698a0.

Tomasko, M. G., and R. A. West (2009), Aerosols in Titan's atmosphere, in *Titan From Cassini-Huygens*, edited by R. H. Brown, J.-P. Lebreton, and J. H. Waite, pp. 297–321, Springer, New York, doi:10.1007/978-1-4020-9215-2_12.

Tomasko, M. G., B. Bézard, L. Doose, S. Engel, E. Karkoschka, and E. S. Vinatier (2008a), Heat balance in Titan's atmosphere, *Planet. Space Sci.*, *56*, 648–659, doi:10.1016/j.pss.2007.10.012.

Tomasko, M. G., L. Doose, S. Engel, L. E. Dafoe, R. West, M. Lemmon, E. Karkoschka, and C. See (2008b), A model of Titan's aerosols based on measurements made inside the atmosphere, *Planet. Space Sci.*, *56*, 669–707, doi:10.1016/j.pss.2007.11.019.

Tomasko, M. G., L. Doose, L. Dafoe, and C. See (2009), Limits on the size of aerosols from measurements of linear polarization in Titan's atmosphere, *Icarus*, *204*, 271–283, doi:10.1016/j.icarus.2009.05.034.

Waite, J. H., Jr., D. T. Young, T. E. Cravens, A. J. Coates, F. J. Crary, B. Magee, and J. Westlake (2007), The process of tholin formation in Titan's upper atmosphere, *Science*, *316*, 870–875, doi:10.1126/science.1139727.

J. Balloch, P. Dumont, T. Ray, and R. A. West, Jet Propulsion Laboratory, California Institute of Technology, 4800 Oak Grove Dr., Pasadena, CA 91109, USA. (robert.a.west@jpl.nasa.gov)

P. Lavvas, Lunar and Planetary Laboratory, University of Arizona, 1629 E. University Blvd., Tucson, AZ 85721-0092, USA.

R. Lorenz and E. P. Turtle, Johns Hopkins University Applied Physics Laboratory, 11100 Johns Hopkins Rd., Laurel, MD 20723, USA.

P. Rannou, GSMA, UMR 6089, CNRS, Université de Reims Champagne-Ardenne, BP 1039, F-51687 Reims CEDEX 2, France.